Numerical computation of invariant densities of linear control systems driven by multiplicative white noise

FRITZ COLONIUS*†, TOBIAS GAYER† and IAKOVOS MATSIKIS†‡

†Institut für Mathematik, Universität Augsburg, D-86135 Augsburg, Germany
‡School of Mathematical Sciences, University of Exeter, Exeter EX4 4QE, UK

For the 3-D linear oscillator with damping and disturbed by multiplicative white noise, we numerically compute the unique invariant density of the associated system obtained by projection onto the unit sphere. We show how varying feedback gains and noise intensities affect the corresponding density and consequently the stability properties.

1. Introduction

This paper presents a numerical study of linear feedback systems in $\mathbb{R}^d$ with multiplicative white noise of the form

$$\dot{x} = Ax + bu + \sigma A_1 x \circ dW(t) \tag{1}$$

$$y = c^T x \tag{2}$$

where $x \in \mathbb{R}^d$, $A, A_j \in \mathbb{R}^{d\times d}$, $b, c \in \mathbb{R}^d$, σW is the Wiener process with intensity $\sigma \in \mathbb{R}$, and $\circ$ means that (1) is interpreted as a Stratonovich stochastic differential equation. Output feedback

$$u = -ky, \tag{3}$$

where $k \in \mathbb{R}$ is a gain parameter, yields the feedback system

$$dx = (A - kbc^T)x\,dt + \sigma A_1 x \circ dW(t). \tag{4}$$

It is well known that basic properties of this linear stochastic differential equation can be described by considering its projection to the unit sphere (or, more precisely, to projective space $\mathbb{P}^{d-1}$) and the corresponding invariant measure. In particular, this is true for the Lyapunov exponents (given by Khasminskii's formula) (Arnold *et al.* 1983, 1986a). The purpose of the present paper is to present some results illustrating the influence of the gain parameter k and the intensity σ of the noise on the invariant measure. For a two dimensional system, Crauel *et al.* (2003) presented asymptotic results for high gain, i.e., for $k \to \infty$. For dimensions $d > 2$ the used expansion is not readily available since it is based on an analytical solution of the Fokker–Planck equation (cp. Remark 3.3 in (Crauel *et al.* 2003). For $d=3$, we will instead use a numerical approach for the computation of the invariant measure on $\mathbb{P}^2$. In particular, we discuss the third order oscillators

$$x^{(3)} - a\ddot{x} - b\dot{x} - cx = u + \sigma x \circ dW \tag{5}$$

and

$$x^{(3)} - a\ddot{x} - b\dot{x} - cx = u + \sigma \dot{x} \circ dW, \tag{6}$$

with output feedback

$$u = -kx.$$

For the induced system on projective space $\mathbb{P}^2$, there is a unique invariant measure μ and it has support equal to $\mathbb{P}^2$. Using polar coordinates, we determine μ by discretization of this space and simulation of the resulting Markov chain. This is done with the help of data

*Corresponding author. Email: fritz.colonius@math.uni-augsburg.de

structures provided by GAIO (Global Analysis of Invariant Objects), a program developed by Dellnitz *et al.* (see Dellnitz *et al.* (1997), Dellnitz and Junge (2002)). Then the density of the invariant measure can be visualized (using MATLAB).

For deterministic systems it is well known that increasing the gain parameter k forces one, some, or even all of the eigenvalues to decrease relatively to the values of the gain. As a consequence the system will be pushed towards the eigendirection associated with the greatest positive eigenvalue (or least negative if all the eigenvalues become negative). A natural invariant measure for this system is a Dirac measure concentrated in this eigendirection.

The numerical simulations show a similar behaviour for small noise intensity. Here the induced system on projective space will move faster and faster towards the least stable (or most unstable) eigendirection, hence the invariant measure will peak near this eigendirection. Increase of the noise intensity has an opposite effect: The invariant measure spreads out on projective space. Thus for higher noise intensity higher gains are necessary in order to obtain peaking near the least stable eigendirection (or, for smaller gains, less noise intensity is necessary in order to spread out the invariant measure).

The contents of the paper are as follows: In §2 we recall results on the projected system on $\mathbb{P}^{d-1}$, in particular, the relevant Lie algebraic conditions. We verify that they are satisfied for (5) and (6) and indicate the parametrisation by polar coordinates. Section 3 describes the numerical method. Section 4 illustrates this by application to a simple second order oscillator, and §5 presents results for the third order oscillators.

2. Projecting onto the unit sphere

In this section, we first recall some general results on Lyapunov exponents, that is, unique existence of invariant measures for the induced system on projective space and Lie algebraic conditions from Arnold *et al.* (1986). Then we verify that these Lie algebraic conditions are satisfied for the oscillators (5) and (6).

Consider a linear stochastic differential equation in $\mathbb{R}^d$ given by

$$dx_t = Ax_t dt + Dx_t \circ dW(t)$$

with $A, D \in \mathbb{R}^{d\times d}$. Defining

$$s = \frac{x}{|x|} \in \mathbb{S}^{d-1} := \{y \in \mathbb{R}^d,\ |y| = 1\},$$

this induces a (non-linear) stochastic differential equation on the sphere $\mathbb{S}^{d-1}$ given by

$$ds = h_A(s)\,dt + h_D(s) \circ dW(t); \tag{7}$$

here $h_A(s) = As - (s, As)s$ and $h_D(s) = Ds - (s, Ds)s$. We note that this also induces a stochastic differential equation on projective space $\mathbb{P}^{d-1}$ which can be obtained by identifying opposite points on the sphere.

We cite the following theorem from (Arnold *et al.* 1986); see also Arnold (1998), Theorem 6.2.16.

Theorem: *Suppose the vector fields h_A and h_D induced by (7) on $\mathbb{S}^{d-1}$ satisfy the following hypoellipticity condition*

$$\dim LA(h_A, h_D)(s) = d - 1 \quad \textit{forall } s \in \mathbb{S}^{d-1}.$$

Then there exists a unique invariant measure on $\mathbb{P}^{d-1}$; it has C^∞ density and the maximal Lyapunov exponent for (7) is constant a.s. □

Thus for the analysis of the oscillators (5) and (6) we have to verify the hypoellipticity condition. We first pass to state space representation

$$dx = \begin{bmatrix} 0 & 1 & 0 \\ 0 & 0 & 1 \\ a & b & c-k \end{bmatrix} x\,dt + \sigma \begin{bmatrix} 0 & 0 & 0 \\ 0 & 0 & 0 \\ 0 & 0 & 1 \end{bmatrix} x \circ dW(t), \tag{8}$$

$$dx = \begin{bmatrix} 0 & 1 & 0 \\ 0 & 0 & 1 \\ a & b & c-k \end{bmatrix} x\,dt + \sigma \begin{bmatrix} 0 & 0 & 0 \\ 0 & 0 & 0 \\ 0 & 1 & 0 \end{bmatrix} x \circ dW(t). \tag{9}$$

Recall that a, b, c and k, σ are fixed real parameters.

Define

$$A = \begin{bmatrix} 0 & 1 & 0 \\ 0 & 0 & 1 \\ a & b & c-k \end{bmatrix}, \quad D_1 = \begin{bmatrix} 0 & 0 & 0 \\ 0 & 0 & 0 \\ 0 & 0 & 1 \end{bmatrix},$$

$$D_2 = \begin{bmatrix} 0 & 0 & 0 \\ 0 & 0 & 0 \\ 0 & 1 & 0 \end{bmatrix}.$$

Then for $j = 1, 2$ the induced systems on $\mathbb{S}^2$ are given by

$$ds = h_A(s)\,dt + \sigma h_{D_j}(s) \circ dW(t) \tag{10}$$

and the hypoellipticity condition becomes

$$\dim LA(h_A, h_{D_j})(s) = 2, \quad \text{for all } s \in \mathbb{S}^2.$$

Moreover, the maximal Lyapunov exponent for (8) and (9) is given by Kashminskii's formula as

$$\lambda = \int_{\mathbb{S}^2} \left((s, As) + \frac{1}{2} \left(\left(D_j + D_j^T \right) s, D_j s \right) - (s, D_j s)^2 \right) \rho(s)\, ds, \tag{11}$$

where $\rho(s)$ denotes the invariant density on $\mathbb{S}^2$ and ds the Lebesgue measure on $\mathbb{S}^2$, and where D_j^T corresponds to the transpose matrix of D_j. A sufficient condition for uniqueness of the invariant measure is that the subspace generated by evaluating the corresponding linear vector fields in $\mathbb{R}^3$ have full dimensions. The following lemma shows that this is indeed the case.

Lemma 2.1: *Suppose that for the systems* (8) *and* (9) *the coefficient* $\alpha \neq 0$. *Then for* $j = 1, 2$ *and every* $x \in \mathbb{R}^3 \backslash \{0\}$

$$\dim LA\{Ax, D_j x\}(x) = 3.$$

Proof: We first treat the case $LA\{Ax, D_1 x\}$ where the vector fields Ax and $D_1 x$ are given by

$$Ax = \begin{pmatrix} x_2 \\ x_3 \\ ax_1 + bx_2 + (c-k)x_3 \end{pmatrix}, \quad D_1 x = \begin{pmatrix} 0 \\ 0 \\ x_3 \end{pmatrix}. \tag{12}$$

We compute the Lie bracket

$$[Ax, D_1 x] = (D_1 A - A D_1)x = \begin{pmatrix} 0 & 0 & 0 \\ 0 & 0 & -1 \\ a & b & 0 \end{pmatrix} x = \begin{pmatrix} 0 \\ -x_3 \\ ax_1 + bx_2 \end{pmatrix}.$$

Thus for $x_2 \neq 0$ and $x_3 \neq 0$ the span is equal to $\mathbb{R}^3$. We further compute

$$\begin{aligned} &[Ax, [Ax, D_1 x]] \\ &= [A, [A, D_1]]x = ([A, D_1]A - A[A, D_1])x \\ &= \begin{pmatrix} 0 & 0 & 1 \\ -2a & -2b & -(c-k) \\ -a(c-k) & a - b(c-k) & 2b \end{pmatrix} x \\ &= \begin{pmatrix} x_3 \\ -2ax_1 - 2bx_2 - (c-k)x_3 \\ -a(c-k)x_1 - (b(c-k) - a)x_2 + 2bx_3 \end{pmatrix}. \end{aligned}$$

If $x_1 = x_2 = 0$, then $x_3 \neq 0$ since $x \in \mathbb{R}^3 \backslash \{0\}$. Hence (12) and the Lie bracket above yields three independent directions. Analogously, the assertion follows if $x_1 = x_3 = 0$. It remains to discuss the case $x_2 = x_3 = 0$ and hence $x_1 \neq 0$.

Since $a \neq 0$, Ax and the Lie bracket above provide two independent directions. In order to find a third independent direction, we compute

$$[A, [A, [A, D_1]]] = \begin{pmatrix} 3a & 3b & 2(c-k) \\ 0 & -3a & -4b - (c-k)^2 \\ 4ab + a(c-k)^2 & \begin{cases} 4b^2 - 2a(c-k) \\ +b(c-k)^2 \end{cases} & 0 \end{pmatrix}$$

and hence

$$[A, [A, [A, D_1]]]x = \begin{pmatrix} -3ax_1 - 3bx_2 - 2(c-k)x_3 \\ 3ax_2 + (4b + (c-k)^2)x_3 \\ -4abx_1 + (-4b^2 + 2a(c-k) - b(c-k)^2)x_2 \end{pmatrix}.$$

This provides a direction independent of Ax and $[A, [A, D_1]]x$. Therefore the first part of the lemma is proved.

We proceed in exactly the same manner for the second case involving the diffusion matrix D_2. Here

$$Ax = \begin{pmatrix} x_2 \\ x_3 \\ ax_1 + bx_2 + (c-k)x_3 \end{pmatrix}, \quad D_2 x = \begin{pmatrix} 0 \\ 0 \\ x_2 \end{pmatrix}.$$

We compute the first bracket of A and D_2 as

$$[A, D_2]x = (D_2 A - A D_2)x = \begin{pmatrix} 0 \\ -x_2 \\ -(c-k)x_2 + x_3 \end{pmatrix}.$$

These three vectors provide us with three independent directions, as long as $x_2 \neq 0$. If $x_2 = 0$ and $x_3 \neq 0$, we have two independent directions

$$\begin{pmatrix} 0 \\ x_3 \\ ax_1 + (c-k)x_3 \end{pmatrix}, \begin{pmatrix} 0 \\ 0 \\ x_3 \end{pmatrix}.$$

If $x_2 = x_3 = 0$, we only have the direction

$$Ax = \begin{pmatrix} 0 \\ 0 \\ ax_1 \end{pmatrix}.$$

We further compute

$$[A,[A,D_2]]x = \begin{pmatrix} x_2 \\ (c-k)x_2 - 2x_3 \\ ax_1 + \big(2b + (c-k)^2\big)x_2 - (c-k)x_3 \end{pmatrix}$$

and

$$[A,[A,[A,D_2]]]x = \begin{pmatrix} -(c-k)x_2 + 3x_3 \\ -3ax_1 - \big(4b + (c-k)^2\big)x_2 \\ \begin{Bmatrix} -2a(c-k)x_1 - \big(4b(c-k) \\ +(c-k)^3\big)x_2 + \big(4b + (c-k)^2\big)x_3 \end{Bmatrix} \end{pmatrix}, \tag{13}$$

and, finally,

$$[A,[A,[A,[A,D_2]]]]x = \begin{pmatrix} 6ax_1 + \big(7b + (c-k)^2\big)x_2 + 2(c-k)x_3 \\ z_1x_1 + z_2x_2 - z_3x_3 \\ y_1x_1 + y_2x_2 - y_3x_3 \end{pmatrix}, \tag{14}$$

where $z_1 = 2a(c-k)$, $z_2 = (4b(c-k) + (c-k)^3 - 3a)$, $z_3 = (8b + 2(c-k)^2)$, $y_1 = (7ab + 3a(c-k)^2)$, $y_2 = (-a(c-k) + 8b^2 + 6b(c-k)^2 + (c-k)^4)$, $y_3 = (3a + 4b(c-k) + (c-k)^3)$.

If $x_2 = x_3 = 0$, then, in addition to Ax, we obtain the two independent directions (13) and (14).

The case $x_2 = 0$, $x_3 \neq 0$ is covered from the directions given by Ax, $[A,D_2]x$, and $[A,[A,[A,D_2]]]x$. This completes the proof. □

This lemma, together with the theorem cited above shows that the induced equations on projective space possess unique invariant measures. The C^∞ densities associated with these measures can be obtained as suitably normalized solutions of the corresponding Fokker–Planck equations in projective space. In some cases (for $d=2$) this even admits an analytical description, see (Crauel *et al.* 2003; Arnold *et al.* 1996). In general, one may use numerical procedures for partial differential equations to solve the Fokker–Planck equation.

Below we follow another numerical approach based on discretizing the state space and then using a Monte–Carlo approach. It will be convenient to introduce angular coordinates for the considered systems in $\mathbb{S}^1$ and $\mathbb{S}^2$ (see §6 for some comments on this choice).

For the stochastic differential equations (10) we get

$$h_A(s) = \begin{pmatrix} s_2 - s_1(s,As) \\ s_3 - s_2(s,As) \\ as_1 + bs_2 + (c-k)s_3 - s_3(s,As) \end{pmatrix},$$

and

$$h_{D_1}(s) = \sigma \begin{pmatrix} -s_1(s,D_1s) \\ -s_2(s,D_1s) \\ s_3 - s_3(s,D_1s) \end{pmatrix},$$

$$h_{D_2}(s) = \sigma \begin{pmatrix} -s_1(s,D_2s) \\ -s_2(s,D_2s) \\ s_2 - s_3(s,D_2s) \end{pmatrix},$$

with

$$(s,As) = s_1s_2 + s_2s_3 + as_3s_1 + bs_3s_2 + (c-k)s_3^2,$$

$$(s,D_1s) = s_3^2$$

and

$$(s,D_2s) = s_3s_2.$$

On the unit sphere the Cartesian coordinates are $s = (s_1,s_2,s_3)^T$ and changing to angular coordinates $s = (\cos\phi\sin\theta, \sin\phi\sin\theta, \cos\theta)^T$ with $\phi \in [0,2\pi)$ and $\theta \in [0,\pi/2)$ (where $\theta \in [0,\pi/2)$ since the density is periodic; the lower half of the unit sphere can be recovered by multiplying with -1) gives

$$d\theta = -\frac{ds_3}{\sin\theta},\quad d\phi = \frac{ds_2}{\sin\theta\cos\phi} - \cot\theta\tan\phi\,d\theta.$$

These equations produce the final transformation with respect to the angles θ and ϕ, of equations (10) with $j=1,2$. Abbreviate

$$M_A = \sin^2\theta\cos\phi\sin\phi + a\sin\theta\cos\phi\cos\theta + (1+b)\sin\theta\sin\phi\cos\theta + (c-k)\cos^2\theta.$$

We compute for $j=1$

$$d\theta = -\Big(a\cos\phi + b\sin\phi + (c-k)\cot\theta - \cot\theta M_A\Big)dt - \sigma\Big(\cot\theta - \cot\theta\cos^2\theta\Big)\circ dW(t),$$

$$d\phi = \left(\frac{\cot\theta}{\cos\phi} - \tan\phi M_A + a\cot\theta\sin\phi + b\frac{\cot\theta\sin^2\phi}{\cos\phi} + (c-k)\cot^2\theta\tan\phi - \cot^2\theta\tan\phi M_A\right)dt - \sigma\left(\tan\phi\cos^2\theta - \cot^2\theta\tan\phi + \cot^2\theta\tan\phi\cos^2\theta\right) \circ dW(t)$$

and for $j=2$ we similarly find

$$d\theta = -\left(a\cos\phi + b\sin\phi + (c-k)\cot\theta - \cot\theta M_A\right)dt - \sigma\left(\sin\phi - \sin\phi\cos^2\theta\right) \circ dW(t),$$

$$d\phi = \left(\frac{\cot\theta}{\cos\phi} - \tan\phi M_A + a\cot\theta\sin\phi + b\frac{\cot\theta\sin^2\phi}{\cos\phi} + (c-k)\cot^2\theta\tan\phi - \cot^2\theta\tan\phi M_A\right)dt - \sigma\left(\frac{\sin\theta\sin^2\phi\cos\theta}{\cos\phi} - \frac{\cot\theta\sin^2\phi}{\cos\phi} + \frac{\sin^2\phi\cos^3\theta}{\sin\theta\cos\phi}\right) \circ dW(t).$$

3. Numerical approximation of the invariant densities

In this section we discuss a numerical method for approximating the unique invariant density in projective space. More details about the numerical details can be found in Gayer (2003). We first discretize the state space by dividing it into 'boxes'. For the projected system in $\mathbb{S}^2$ we use angular coordinates. Identifying opposite points on the sphere we obtain the projective space $\mathbb{P}^2$. For this space we use coordinates in $K = [0, 2\pi] \times [0, \pi/2]$, which is the upper half of the unit sphere. The computation of the invariant density on this space is based on the discretization of the Frobenius–Perron operator defined on the space of probability measures on $\mathbb{R}^2$. Choose a discretization time $T > 0$ and define a partition of K into finitely many boxes B_i. Then compute the transition probabilities

$$p_{ij} := \frac{1}{m(B_i)}\int_{B_i} P(T, x, B_j)\,dx$$

for the ensuing discretized system averaged over the box covering. Here $m(\cdot)$ denotes the Lebesgue measure. The transition matrix $P := (p_{ij}) \in \mathbb{R}^{(N+1)\times(N+1)}$ is row stochastic.

This partition is numerically very convenient; for the generation of the boxes we rely on subdivision techniques for the numerical analysis of dynamical systems developed by Dellnitz *et al.* (see (Dellnitz and Hohmann 1997; Dellnitz and Junge 2002)). For the approximation of the dynamics on this box partition, we create a Markov chain with finitely many states each of which symbolizes one box. The transition probabilities from one state to the other are computed by Monte Carlo simulation; here we use a stochastic Runge–Kutta technique of order four (see e.g. Kloeden and Platen 1992).

More specifically, s_2 starting points x^k are picked in each box B_i. From each starting point, the solution is approximated for all samples $\hat{\eta}^l$ generating $s_1 s_2$ target points $\hat{\varphi}(T, x^k, \hat{\eta}^l)$. The transition function from box B_i to B_j is then approximated by

$$p_{ij} = \frac{1}{m(B_i)}\int_{B_i} P(T, x, \eta_t)\,dx \approx \frac{1}{s_1 s_2}\sum_{l}^{s_1}\sum_{k}^{s_2} \chi_{B_j}\left(\hat{\varphi}(T, x^k, \hat{\eta}^l)\right).$$

The question as to how many starting points, boxes, and sample paths of the background process should be used depends on the properties of the system, the time length T, and the box size-and, of course, on the available computing resources.

This yields the transition matrix of the Markov chain, which in turn allows the computation of the stationary density which is represented as a normalized eigenvector of the discretized Frobenius–Perron operator associated with the eigenvalue one. Thus an approximation to a fixed point of the Frobenius–Perron operator is obtained.

Remark 3.1: The universally applied idea of Monte-Carlo simulations goes back to Ulam, Metropolis, and von Neumann (see Metropolis and Ulam (1949)). Although many sophisticated variants for different disciplines have been developed in the meanwhile, there are no general error estimates available.

Remark 3.2: For further information on results concerning the convergence of the above approximations we refer the reader to Dellnitz and Junge (2002), Ding *et al.* (1993) and Hunt (1994) for the deterministic case and to Imkeller and Kloeden (2003) for the approximation of invariant measures for random dynamical systems.

Remark 3.3: We note that numerical methods for the computation of invariant measures are frequently used

in stochastic mechanics. We only mention Karch and Wedig (1995), Griesbaum (1999). Griesbaum in particular approximates the invariant density on the sphere and computes Lyapunov exponents, similarly as above. His approximation is either based on Monte-Carlo simulations or on a numerical solution of the Fokker–Planck equation in angular coordinates; then he uses a Fourier series expansion causing difficulties in dimension larger than two. Results for certain systems in dimension two, and three and four are included.

4. Examples, 2-D case

In this section we illustrate the previous ideas for the following two dimensional stochastic oscillator and with noise acting in a purely skew symmetric way.

$$dx = \begin{pmatrix} 3-k & -4 \\ 1 & -10 \end{pmatrix} x\,dt + \sigma \begin{pmatrix} 0 & -1 \\ 1 & 0 \end{pmatrix} x \circ dW(t). \tag{15}$$

Specifically, we will study the effects of small ($\sigma = 10^{-5}$) and relatively big ($\sigma = 1$) noise on the corresponding invariant measure of (15) for different high gain values.

We adopt the values $a = 3$, $b = -4$, $c = 1$, $d = -10$ for the drift matrix (which we call A_1) because they make the origin of the unperturbed system a saddle and the corresponding root locus is dynamically more interesting.

Remark 4.1: Observe that when noise enters in this skew symmetric way the system for the angle ϕ on $\mathbb{S}^1$ is elliptic and so there is a unique invariant measure.

4.1. *Small noise intensity*

We start by plotting the root locus for the unperturbed equation (15), this is shown in figure 1.

The root locus shows that for $0 < k \leq 9$ there are two real eigenvalues $\lambda_1 \approx -9.69$ and $\lambda_2 \approx 2.69$, which become complex for $9 < k < 17$ and eventually for $k \geq 17$ one converges to minus infinity and the other to $d = -10$. Thus the origin will change from being a saddle to a stable spiral and will eventually become a stable node.

The latter arguments imply that the invariant measure of (15) for $0 < k \leq 9$ will almost be a Dirac measure concentrated in the eigendirection corresponding to λ_2, this is shown in figure 2. (*Here and in the following figures we plot the different values of the density as distances from the unit circle* $\mathbb{S}^1$.) For $9 < k < 17$ the density assumes values different than zero in a wider

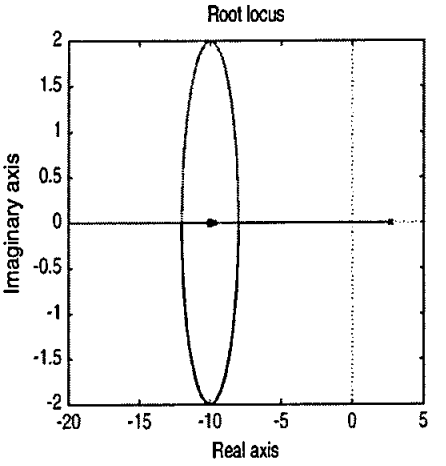

Figure 1. Root locus for A_1.

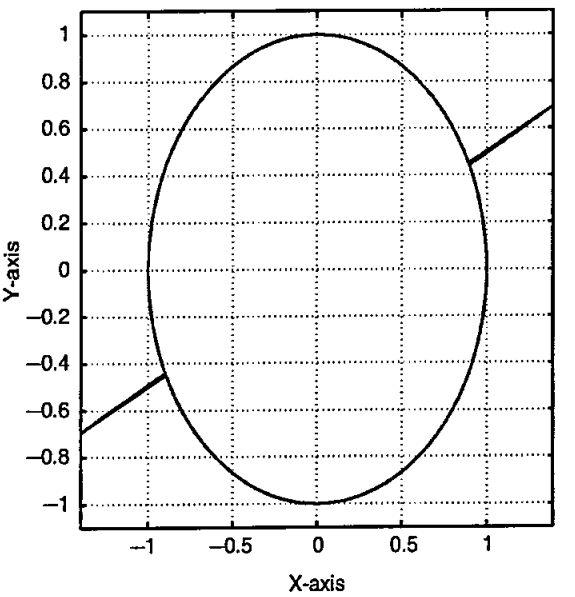

Figure 2. $\sigma = 10^{-5}$ and $k = 9$.

area since the solution becomes a spiral and thus visits some areas of $\mathbb{S}^1$ more than once, figure 3. However, since noise is small, high gain forces the density to concentrate more in one 'box'. This is seen in figure 3 where only one big peak appears.

For $k = 20$, the measure returns to being almost Dirac, figure 4. Increasing k further, noise gradually loses its effect and the measure approximates a Dirac measure concentrated on the north pole, figure 5.

4.2. *Noise intensity* $\sigma = 1$

In this subsection we treat again equation (15), but we increase the noise intensity to one. The smoothing

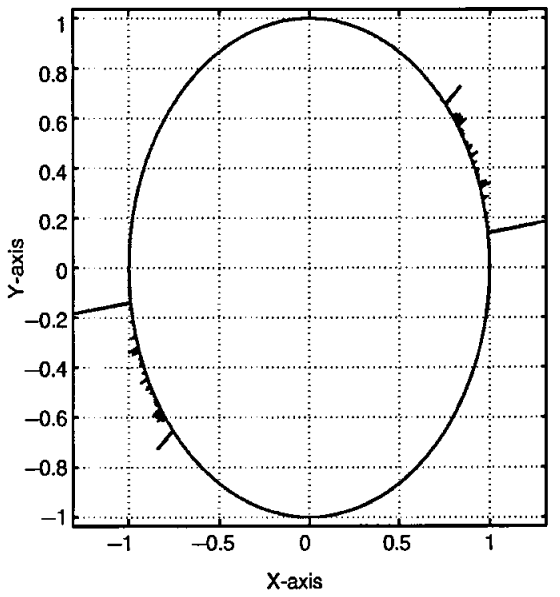

Figure 3. $\sigma = 10^{-5}$ and $k = 10$.

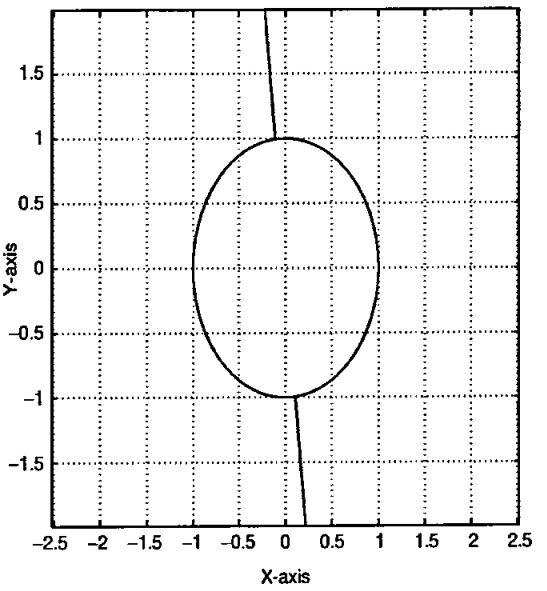

Figure 5. $\sigma = 10^{-5}$ and $k = 50$.

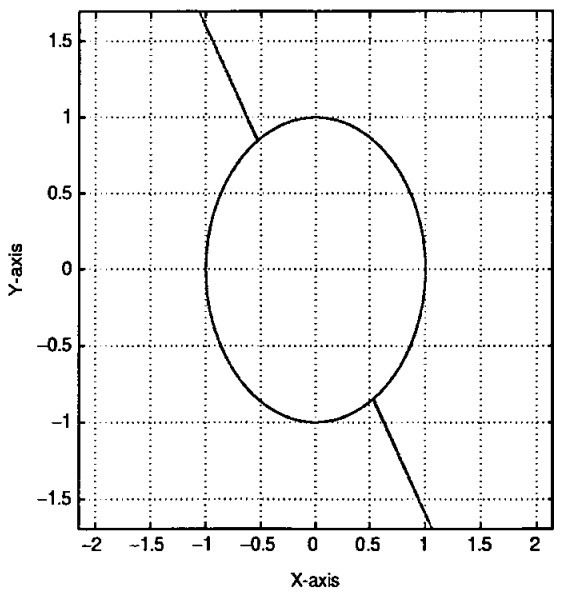

Figure 4. $\sigma = 10^{-5}$ and $k = 20$.

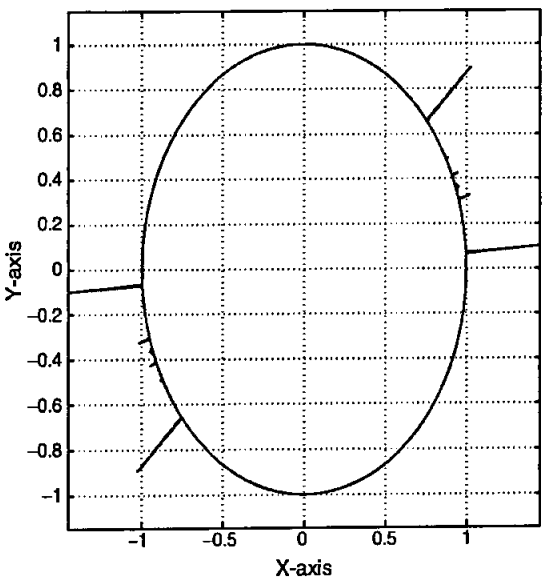

Figure 6. $\sigma = 1$ and $k = 10$.

effect of noise can be viewed in the following two figures which were made using the same configuration as for figures 3 and 5, with the exception that noise intensity was increased.

Observe how the density from peaking at one point in figure 3, 'spreads out' in two big peaks in figure 6. The same happens between figures 5 and 7 where the density from having value almost one for $\sigma = 10^{-5}$ becomes much smaller and spreads uniformly on the surface of $\mathbb{S}^1$.

5. Examples, 3-D case

We now study the combined effect of noise intensity and high gain on the density of the third order linear oscillators (5) and (6). For both equations the drift matrices A coincide. We begin with the root locus of the drift matrix A. Then we study (5) and (6) considering different noise intensities and gains k.

Note: *In contrast to the 2-D case where we plotted the different density values as distances from the surface of* $\mathbb{S}^1$, *here we use grey shades to plot them on* $\mathbb{S}^2$.

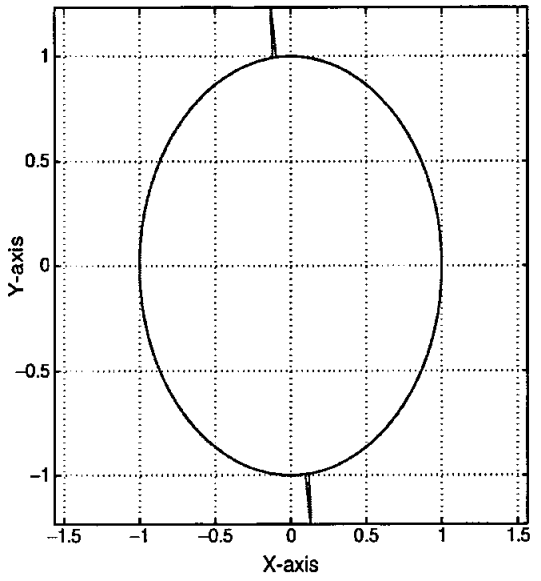

Figure 7. $\sigma = 1$ and $k = 50$.

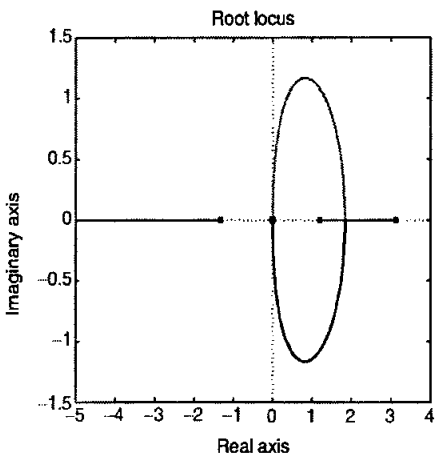

Figure 8. Root locus for A.

5.1. *Small noise intensity*

The root locus for

$$A = \begin{bmatrix} 0 & 1 & 0 \\ 0 & 0 & 1 \\ -5 & 2 & 3-k \end{bmatrix}$$

is plotted in figure 8,

In particular, for $k = 0$ we get three real eigenvalues $\lambda_1 = 3.1284, \lambda_2 = -1.3301$ and $\lambda_3 = 1.2016$. The red line indicates that λ_2 will remain real for all subsequent values of k and will move gradually towards minus infinity. On the other hand, when $k \approx 0.77$ eigenvalues λ_1 and λ_3 become complex and stay complex for all greater values of k.

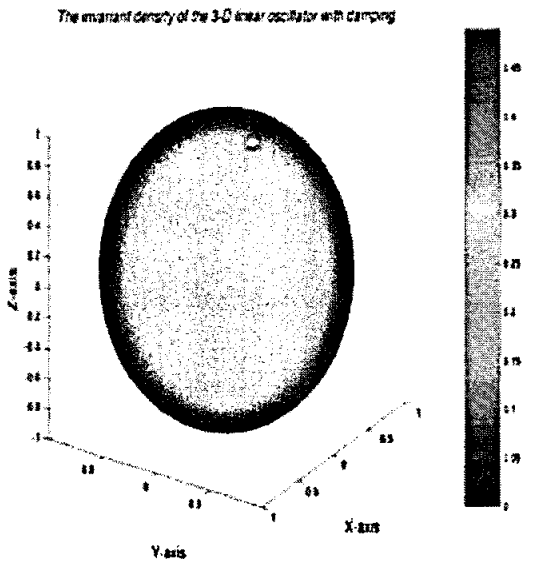

Figure 9. $\sigma = 10^{-6}$ and $k = 0$.

Next we study equation (5) given by

$$dx = \begin{bmatrix} 0 & 1 & 0 \\ 0 & 0 & 1 \\ -5 & 2 & 3-k \end{bmatrix} x\,dt + \sigma \begin{bmatrix} 0 & 0 & 0 \\ 0 & 0 & 0 \\ 0 & 0 & 1 \end{bmatrix} x \circ dW(t), \tag{16}$$

Thus for $k = 0$ we get an almost Dirac measure concentrated in the eigendirection associated with λ_1, this can be seen in figure 9. For $k > 0.77$ the solution of the unperturbed system becomes an unstable spiral and so the peak flattens in figure 10.

Increasing now k to values higher than one forces the solution to oscillate faster since the imaginary parts of λ_1 and λ_3 increase. Therefore the density becomes a 'ring' around $\mathbb{S}^2$ as can be seen in figures 11 and 12.

For $k > 10$ the density will keep on being a 'ring' and eventually become the equator. Observe, however, that for higher values of k the noise affects the system less and so the density concentrates (peaks) more. This is seen in figure 12 where-in the lighter parts-maximal values close to 0.04 are attained in comparison with 0.03 in figure 11.

5.2. *Higher noise intensity*

We now increase the noise intensity to $\sigma = 1$ and compare with the small noise case. Observe in

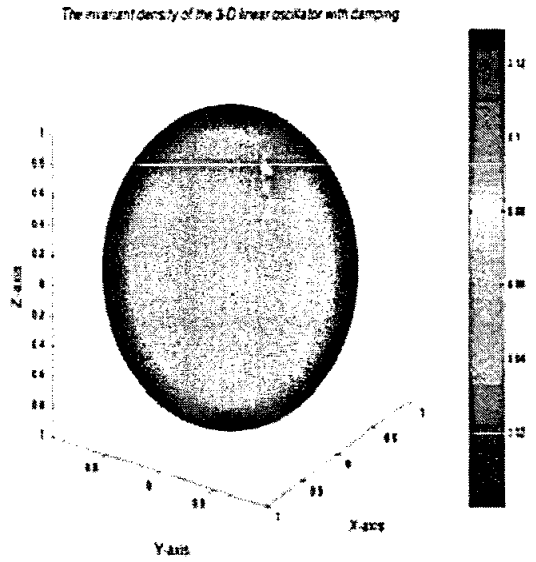

Figure 10. $\sigma = 10^{-6}$ and $k = 1$.

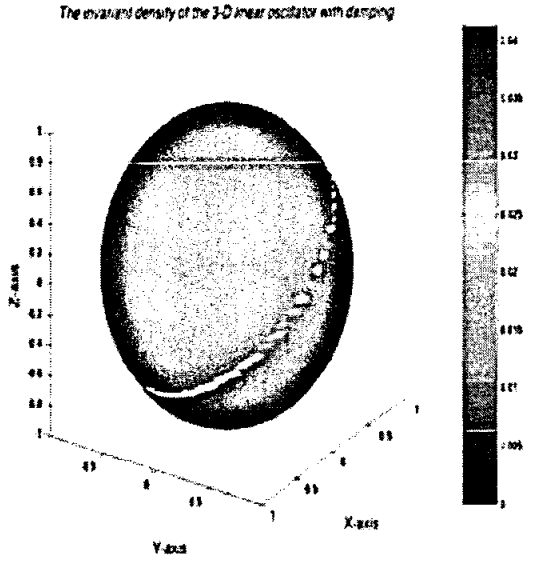

Figure 12. $\sigma = 10^{-6}$ and $k = 10$.

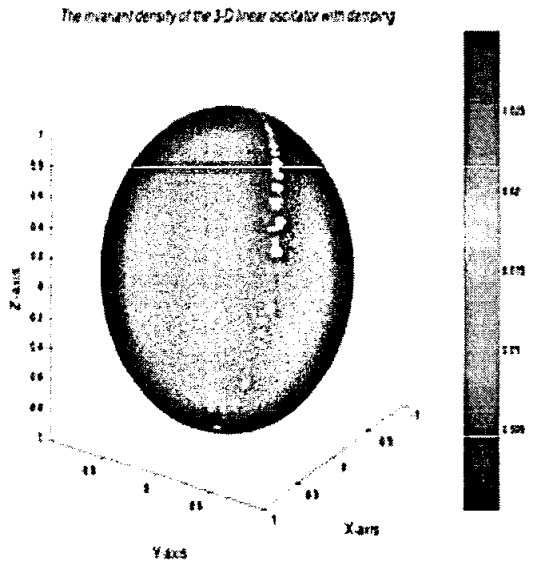

Figure 11. $\sigma = 10^{-6}$ and $k = 3$.

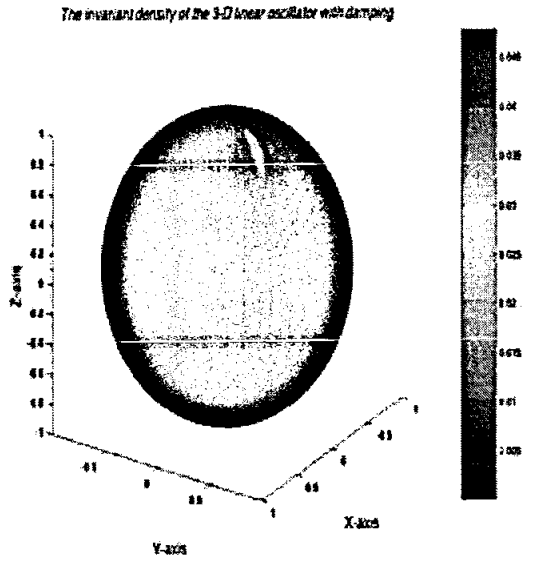

Figure 13. $\sigma = 1$ and $k = 0$.

figures 13–16 how the density spreads out in comparison with the small intensity case. The peaks, for example in figures 11 and 12, disappear.

Before closing this subsection we present figure 17 for $\sigma = 5$ and figure 18 for $\sigma = 20$. Here the smoothing effect of higher noise intensity becomes more visible.

Clearly, the more σ increases for constant k, the more the density flattens around the sphere in a uniform manner.

5.3. *Different diffusions*

Finally, we study what happens to the density function when we switch from equation (5) to equation (6). We use the same drift matrix A for the calculations and noise intensity $\sigma = 1$.

We see that although the quantitative behaviour of the density remains the same as can be easily seen between figures 13, 14 and 19, 20, nevertheless qualitatively the density finds a new area of concentration, figures 15, 16 and 21, 22. This leads us to believe that

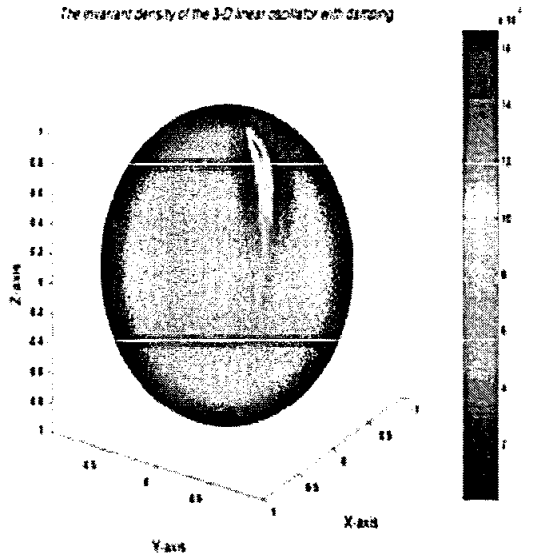

Figure 14. $\sigma = 1$ and $k = 1$.

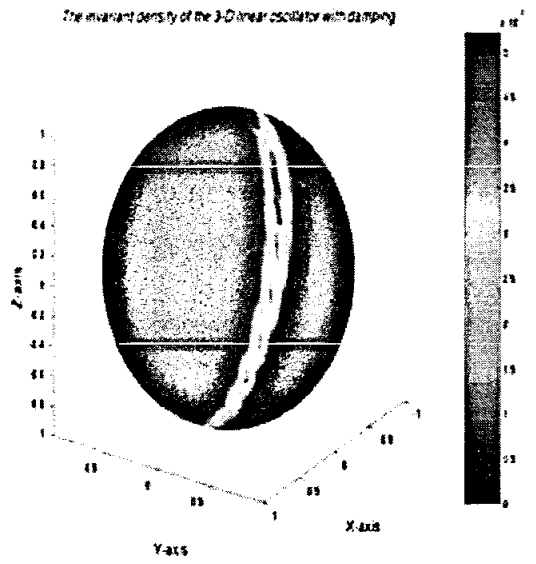

Figure 15. $\sigma = 1$ and $k = 3$.

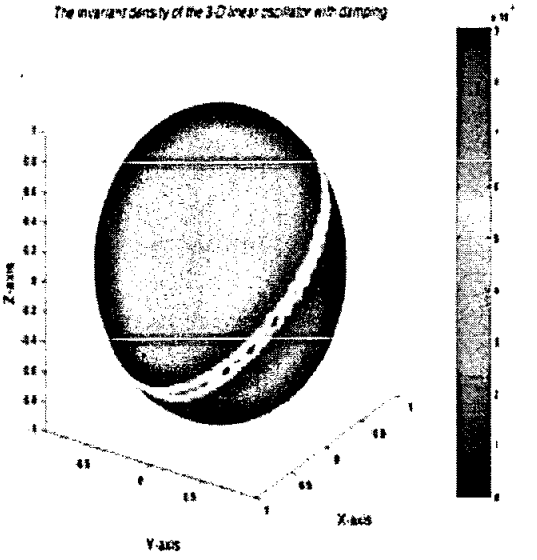

Figure 16. $\sigma = 1$ and $k = 10$.

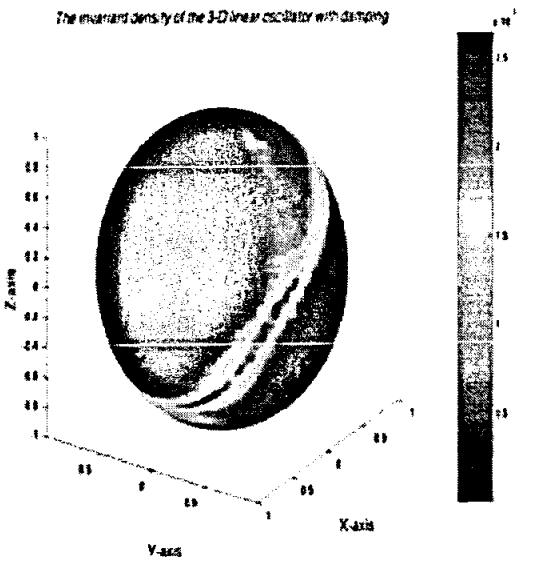

Figure 17. $\sigma = 5$ and $k = 10$.

different mixing of noise significantly alters the properties of the invariant measure when high gain is not big enough to counterbalance the effect of the noise.

5.4. *Application to Lyapunov exponents*

Using the measures we calculated in the previous section, we now compute the Lyapunov exponents λ_{D_1} and λ_{D_2} from equation (11) as functions of high gain and noise intensity. Specifically we plot λ_{D_1, D_2} for $0 \leq k \leq 10$ and for noise intensities $\sigma = 10^{-6}$ and $\sigma = 1$. We start by computing for equation (8) the maximal Lyapunov exponent (11) with respect to the angles (ϕ, θ) on $\mathbb{P}^2$. This gives

$$\lambda_{D_1} = \int_0^{2\pi} \int_0^{\pi/2} \left(\frac{1}{2} \sin 2\phi \sin^2 \theta + \frac{1}{2} \sin 2\theta (\sin \phi + a \cos \phi + b \sin \phi) + (c - k) \cos^2 \theta + \sigma^2 (\cos^2 \theta \sin^2 \theta) \right) \times p(\phi, \theta) d\phi \, d\theta.$$

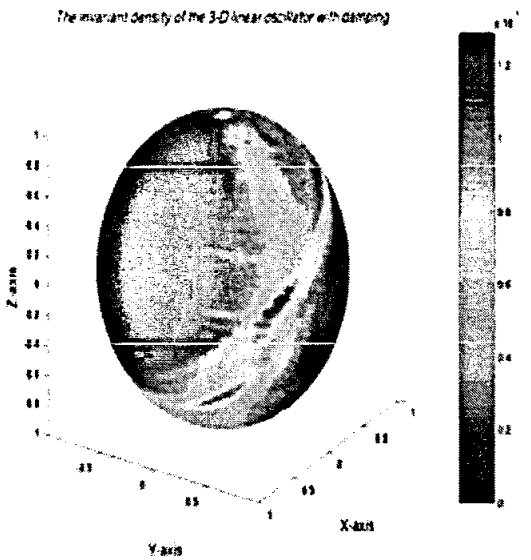

Figure 18. $\sigma=20$ and $k=10$.

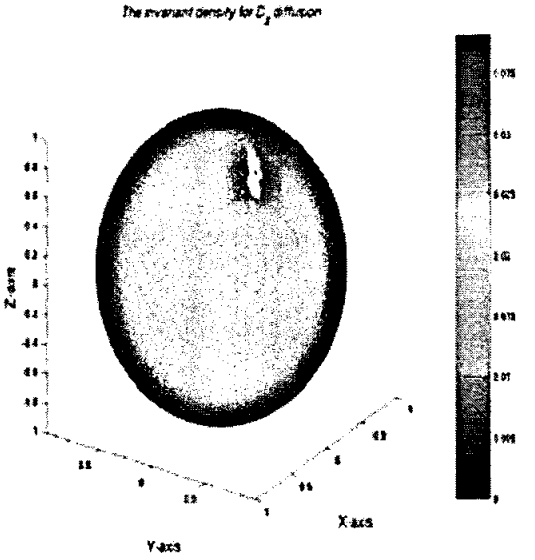

Figure 20. $\sigma=1$ and $k=1$.

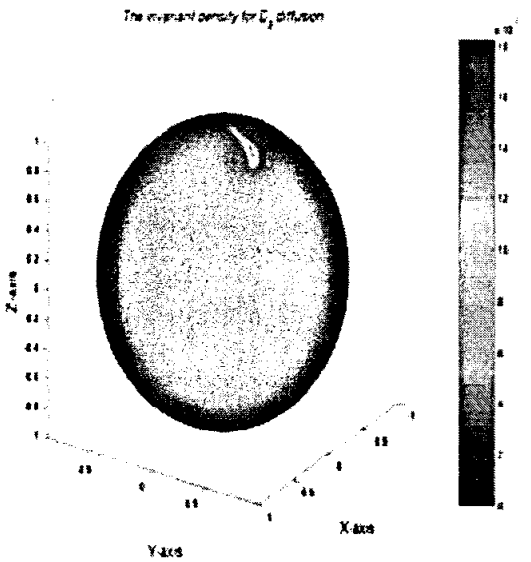

Figure 19. $\sigma=1$ and $k=0$.

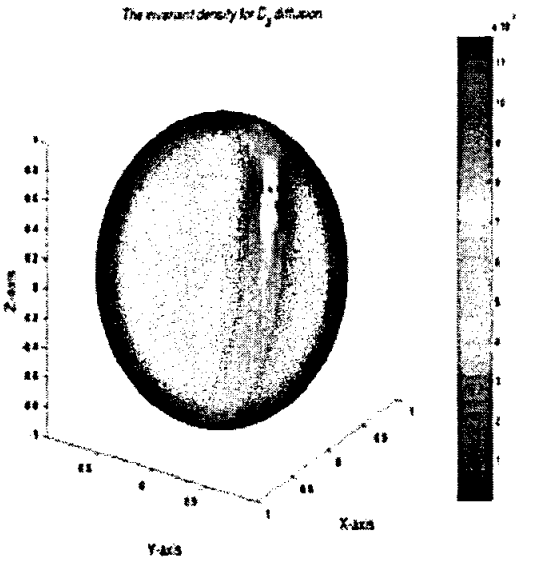

Figure 21. $\sigma=1$ and $k=3$.

Using equation (11) but with different diffusion D_2, we recover the following integral whose solution gives the greatest Lyapunov exponent of equation (9):

$$\lambda_{D_2}=\int_0^{2\pi}\int_0^{\pi/2}\left(\frac{1}{2}\sin 2\phi\sin^2\theta+\frac{1}{2}\sin 2\theta(\sin\phi+a\cos\phi+b\sin\phi)+(c-k)\cos^2\theta+\frac{\sigma^2}{2}(\sin^2\phi\sin^2\theta-2\cos^2\theta\sin^2\phi\sin^2\theta)\right)p(\phi,\theta)d\phi\,d\theta.$$

In figures 23–25 the +-sign corresponds to computed values of .... and the continuous line denotes the real parts of the drift matrices of equations (8) and (9). Both exponents are plotted as k is being increased with step 1 from zero to ten.

Clearly when σ is small, λ_{D_1} (and λ_{D_2}) matches the deterministic exponent, figure 23. Increasing the noise intensity has a destabilizing effect on the system as can be viewed in figure 24, where λ_{D_1} instead of converging fast towards zero is forced to remain positive for a longer period. λ_{D_2} assumes smaller values than the deterministic maximal exponent since the diffusion part coming from D_2 in the Khasminskii formula contributes

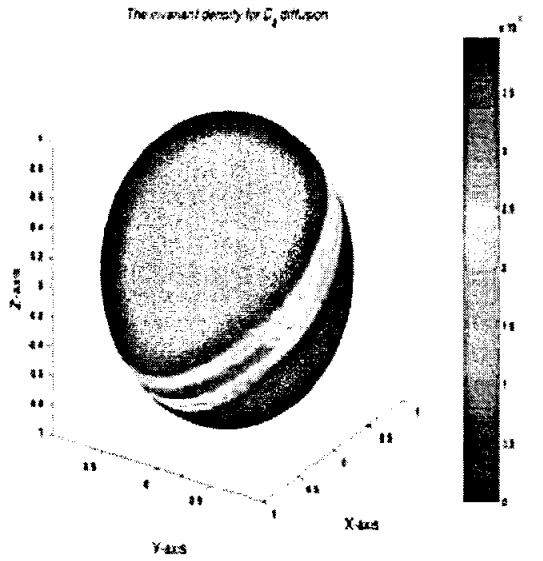

Figure 22. $\sigma = 1$ and $k = 10$.

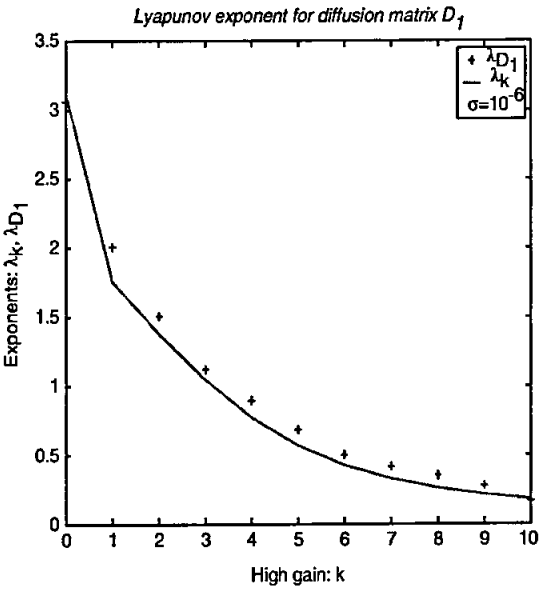

Figure 24. λ_{D_1}, $\sigma = 1$.

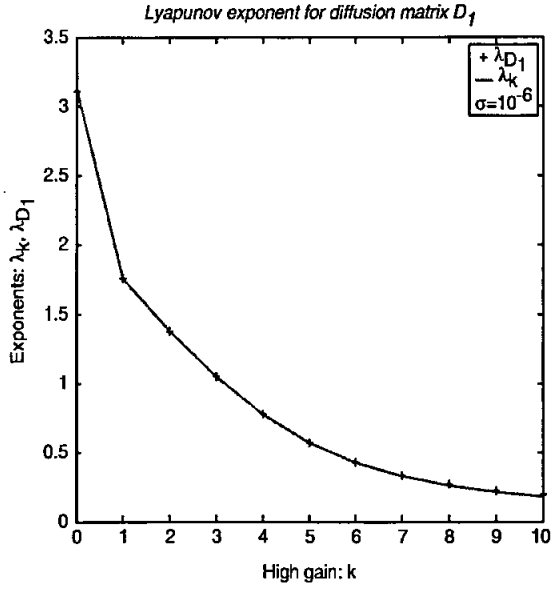

Figure 23. λ_{D_1}, $\sigma = 10^{-6}$.

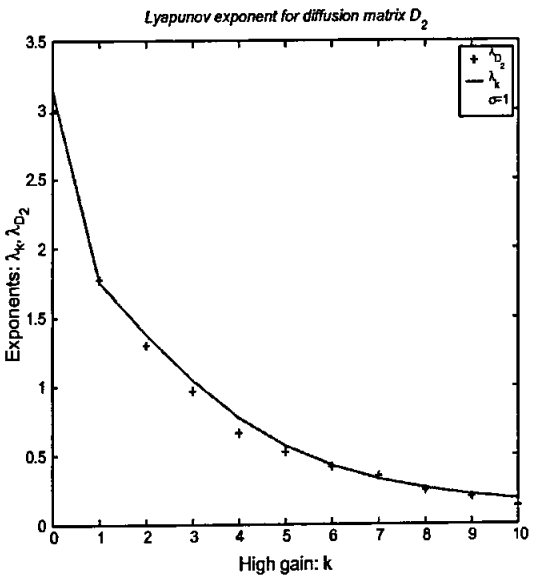

Figure 25. λ_{D_2}, $\sigma = 1$.

negative values. So when noise enters with diffusion D_2 stabilizes in contrast to D_1.

Nevertheless both λ_{D_1} and λ_{D_2} converge to the deterministic exponent for increasing k. This is expected as the invariant measure numerically converges to its deterministic counterpart while k increases.

6. Conclusions

This paper presents numerical results which compare the effects of changes in the gain and in the intensity of noise on the stability behaviour of linear systems measured via the almost sure Lyapunov exponent. In particular, our numerical results show stabilizing and destabilizing effects of noise versus gain changes for three-dimensional systems.

Numerical computation of Lyapunov exponents is a vast field which already for deterministic systems (in the context of chaotic dynamics) poses challenging problems. The approach used here in a stochastic context is based on the Furstenberg–Khasminskii formula determining the Lyapunov exponent by integration with respect to the invariant measure on

projective space. This has the advantage that it also gives information on the directions where the system concentrates. We chose to use a Monte-Carlo method for computation of the invariant measure. Although time-consuming (computation for the 3-D examples took between 3 and 6 hours on a 2.8 GHZ Pentium IV), these methods are, in principle, also applicable in higher dimensional situations. We are not aware of error estimates for these methods. One will expect that this is different for the alternative to compute the invariant measure via the Fokker–Planck equation which determines the invariant measure, since numerical methods for partial differential equations usually include error estimates. However, since this partial differential equation has to be solved numerically on a manifold, the n-sphere, additional problems occur (this becomes e.g. apparent in Griesbaum (1999)). Furthermore, numerical methods for partial differential equations are mainly developed for two or three dimensional state spaces.

Due to the mentioned lack of error estimates, there is a clear need for comparisons of results based on Monte Carlo methods with other techniques for computing invariant densities and/or Lyapunov exponents. Thus the present paper is only a step toward more systematic studies when noise has a stabilizing/destabilizing influence on the system, in particular, in connection with high-gain control.

Acknowledgements

We would like to thank Hans Crauel from the Technical University of Ilmenau, for his various comments and suggestions. Iakovos Matsikis was supported by the Marie-Curie Multipartner project Control Training Site financed by the European Union. We are also grateful to anonymous referees who helped to improve the presentation.

References

L. Arnold, *Random Dynamical Systems*, New York: Springer-Verlag, 1998.

L. Arnold, H. Crauel and V. Wihstutz, "Stabilisation of linear systems by noise", *SIAM J. Control Optimisation*, 21, pp. 451–461, 1983.

L. Arnold, A. Eizenberg and V. Wihstutz, "Large noise asymptotics of invariant measures, with applications to Lyapunov exponents", *Stochastics Rep.*, 59, pp. 71–142, 1996.

L. Arnold, W. Kliemann and E. Oeljeklaus, "Lyapunov exponents of linear stochastic systems", in *Lyapunov Exponents, Proceedings, Bremen* 1984, L. Arnold and V. Wihstutz (Eds), Berlin: Springer-Verlag, 1986a, pp. 85–125.

L. Arnold, E. Oeljeklaus and E. Pardoux, "Almost sure and moment stability for linear Itô equations", in *Lyapunov Exponents, Proceedings, Bremen 1984*, Heidelberg: Springer-Verlag, 1986b, pp. 129–159.

H. Crauel, I. Matsikis and S. Townley, "Noise assisted high-gain stabilization: almost surely or in second mean", *SIAM J. Control Optimisation*, 42(5), pp. 1834–1853, 2003.

M. Dellnitz and A. Hohmann, "A subdivision algorithm for the computation of unstable manifolds and global attractors", *Numer. Math.*, 75, pp. 293–317, 1997.

M. Dellnitz and O. Junge, "Set oriented numerical methods for dynamical systems", in *Handbook of Dynamical Systems III: Towards Applications*, B. Fiedler, G. Ioos and N. Kopell (Eds), Singapore: World Scientific, 2002, pp. 221–264.

M. Dellnitz, A. Hohmann, O. Junge and M. Rumpf, "Exploring invariant sets and invariant measures", *CHAOS: An Interdisciplinary Journal of Nonlinear Science*, 7(2), pp. 221–232, 1997.

J. Ding, Q. Du and T.Y. Li, "High order approximation of the Frobenius–Perron operator", *Applied Mathematics and Computation*, 53, pp. 151—171, 1993.

T. Gayer, "Controlled and perturbed systems under parameter variation", Dissertation Universität Augsburg, Shaker Verlag, Aachen (2003).

R. Griesbaum, "Zur Stabilität dynamischer systeme mit stochastischer parametererregung", Dissertation Universität Karlsruhe, 199, Fortschrittberichte VDI, VDI Verlag, Düsseldorf (1999).

F.Y. Hunt, *A Monte–Carlo Approach to the Approximation of Invariant measures*, Gaithersburg, Random & Computational Dynamics 2 (1994) pp. 111–133.

P. Imkeller and P. Kloeden, "On the computation of invariant measures in random dynamical systems", Stochastics and Dynamics, 3, pp. 247–265, 2003.

G. Karch and W. Wedig, "Computational methods for {L}yapunov exponents and invariant measures", in *Nonlinear Dynamics and Stochastic Mechanics*, W. Kliemann, N. Sri Namachchivaya (Ed.), Boca Raton, Fl.: CRC Press, 1995, pp. 463–477.

P. Kloeden and E. Platen, *Numerical Solutions of Stochastic Differential Equations*, Berlin, Heidelberg: Springer-Verlag, 1992.

N. Metropolis and S. Ulam, "The Monte Carlo method", *J. Amer. Statist. Assoc.*, 44(247), pp. 335–341, 1949.